Available online at www.sciencedirect.com
ScienceDirect
Geochimica et Cosmochimica Acta 74 (2010) 2851–2865
Geochimica et Cosmochimica Acta
www.elsevier.com/locate/gca

U-series disequilibria in suspended river sediments and implication for sediment transfer time in alluvial plains: The case of the Himalayan rivers

M. Granet [a], F. Chabaux [a,*], P. Stille [a], A. Dosseto [b], C. France-Lanord [c], E. Blaes [a]

[a] Laboratoire d'Hydrologie et de Géochimie de Strasbourg, EOST, Université de Strasbourg et CNRS, 1 rue Blessig, 67084 Strasbourg Cedex, France
[b] School of Earth and Environmental Sciences, University of Wollongong, Northfields Avenues, Wollongong, NSW 2522, Australia
[c] Centre de Recherches Pétrographiques et Géochimiques, CNRS, 15 rue Notre Dame des Pauvres, 54501 Vandoeuvre-lès-Nancy, France

Received 1 June 2009; accepted in revised form 10 February 2010; available online 23 February 2010

Abstract

^{238}U–^{234}U–^{230}Th radioactive disequilibria were analyzed in suspended sediments (collected at different depths) from the Ganges River and one of its main tributaries: the Narayani–Gandak River. Results associated with bedload sediment data suggest that uranium-series (U-series) disequilibria in river sediments of the Ganges basin vary with grain size and sampling location. The range of observed U-series disequilibria is explained by a mixing model between a coarse-grained sediment end-member, represented by bedload and bank sediments, and a fine-grained end-member that both originate from Himalaya but undergo different transfer histories within the plain. The coarse-grained sediment end-member transits slowly (i.e. >several 100's ky) in the plain whereas the fine-grained sediment end-member is transferred much faster (<20–25 ky), as indicated by the absence of significant variations in Th isotope composition of the fine-grained sediment end-members. These results show that U-series isotopes can be used to quantify the various transfer times of river sediments of different sizes and infer that there can be an order of magnitude of difference, or more, between the transfer time of suspended and bedload sediments. This underlines that a good knowledge of the proportion of suspended vs. bedload sediments transported in the river is required to accurately assess how fast erosion products are transferred in a catchment and how fast a catchment is likely to respond to external forcing factors.

1. INTRODUCTION

Continental erosion plays an important role in the regulation of atmospheric CO_2 content (e.g., Walker et al., 1981; Berner, 1995; Dupré et al., 2003 and references therein). Thus, it is of prime interest to understand how erosion responds to external forcing factors. To achieve this goal, an important parameter to constrain is the *residence time of sediments in a catchment*. This *sediment residence time* represents the time elapsed since production of solid erosion products from the bedrock, and integrates the storage time in weathering profiles and the transport time in the river (with possible temporary storage in a floodplain). The analysis of uranium-series (U-series) disequilibria in river dissolved and solid loads allows to perform weathering mass balance calculations at the scale of the watersheds and has been used to quantify the sediment residence time in various catchments around the world (e.g., Vigier et al., 2001, 2005; Chabaux et al., 2003a, 2006, 2008; Dosseto et al., 2006a,b,c, 2008a; Granet et al., 2007). These studies, especially when comparing the results of the Amazon river system (Dosseto et al., 2006a,b) with those of the Ganges (Chabaux et al., 2006; Granet et al., 2007), give however quite different time-scales for sedimentary transfer in the alluvial plains: about 20 kyr with the Amazon river and 100 kyr or more for the Ganges. Such a difference

* Corresponding author.
E-mail addresses: fchabaux@unistra.fr, francois.chabaux@eost.u-strasbg.fr (F. Chabaux).

0016-7037/$ - see front matter © 2010 Elsevier Ltd. All rights reserved.
doi:10.1016/j.gca.2010.02.016

could outline differences in geological, climatic, or human settings in these river systems, but could also reflect differences in the rate of sediment transport as a function of grain size, since Dosseto et al. (2006a,b) studied the suspended material of the Amazon rivers whereas Granet et al. (2007) focused on bedload and river bank coarse sediments in the Ganges rivers. In this study, we propose to test this hypothesis by investigating the U-series isotope composition of river suspended sediments. We use the natural granulometric and mineralogical sorting done by the river by analyzing sediments collected at different depths of the water column. This approach is applied to the Ganges river system where sediments have been collected at different locations in the Ganges plain, from the front of the Himalaya High Range to the outlet in the Indian plain.

2. SAMPLING LOCATION AND MAIN MINERALOGICAL AND GEOCHEMICAL SEDIMENT CHARACTERISTICS

Sediments have been collected at three different locations along the Ganges river and at three locations of one of its main tributary named "Narayani" at the front of the Himalaya High Range and "Gandak" in the Indian plain. Sampling locations and their corresponding numbers are reported in Fig. 1. The Narayani samples (#1, Fig. 1) have been collected just downstream the transition between the Himalayan range and the alluvial plain, whereas the Gandak samples (#2 and #3, Fig. 1) have been collected further downstream in the alluvial plain. At each sampling location, suspended, bedload and/or bank sediments were collected. Bedload sediments were sampled in a low regime part of the river. River bank sediments were collected at several locations of a same sampling station in order to integrate a total surface of a few square meters and were mixed together and homogenized (Galy, 1999). Suspended materials were collected in the river main channel during several monsoon sampling campaigns undertaken since 2001. For the three Ganges sampling locations, and one of the Narayani–Gandak locations, suspended sediments were collected at different depths of the water column by using a polypropylene bottle, ballasted and equipped with a depth probe (a detailed description of the sampling procedure is given in Galy (2007)). The sampling depth given in Table 1 corresponds to the average depth recorded during the filling of the bottle and may fluctuate by ±0.5 m. For the sampling site of the Gandak river where no suspended sediments have been collected during monsoon period (#2, Fig. 1), we analyzed clayey bank sediments assumed to represent average fine deposits transported during monsoon period.

As presented in Galy (1999, 2007), the river sediment load in the Ganges basin is characterized by a wide range of mean grain size: from a few μm for suspended materials to approximatively 500 μm for bedload sediments. Regardless the sediment grain size, quartz and micas are the most abundant minerals and represent more than 50% of the mineralogical composition of the sediments. Other minerals are feldspars, chlorite and smectite, with a variable proportion of carbonates (calcite, dolomite). As detailed in Galy et al. (2007), the sedimentary load strongly increases with sampling depth in the water column. For instance, for the Narayani sampling location (#1, Fig. 1), it increases from about 3 g/L in surface waters to 10 g/L in bottom waters.

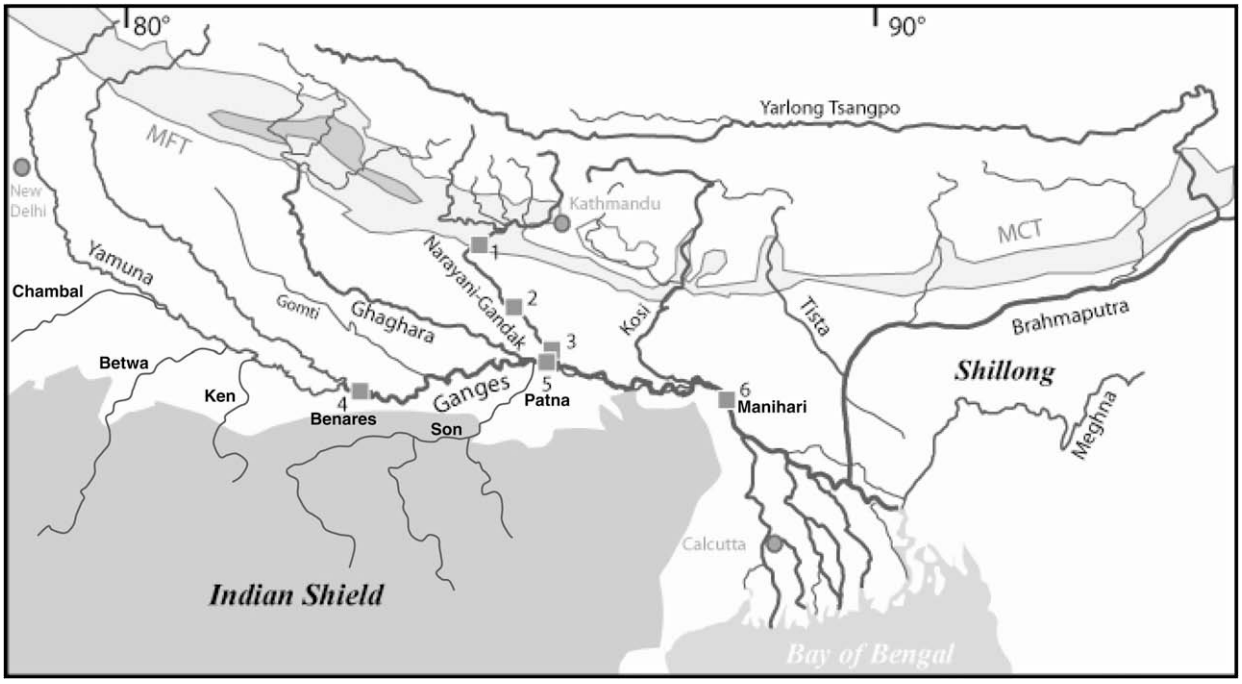

Fig. 1. Map of the Ganges River basin and locations of river sampling, modified from Chabaux et al. (2001). MCT = Main Central Thrust. MFT = Main Frontal Thrust. Location numbers are those given in Table 1.

Table 1
U-series isotope data, Al_2O_3/SiO_2 and Fe_2O_3/SiO_2 ratios for the sediments of the Ganges and Narayani–Gandak rivers.

	Type	Sampling date	Position on the map	Average depth (m)	U (ppm)	Th (ppm)	($^{238}U/^{232}Th$)	($^{230}Th/^{232}Th$)	($^{230}Th/^{238}U$)	($^{234}U/^{238}U$)	Al_2O_3/SiO_2	Fe_2O_3/SiO_2
Pebbles					3.68	16.7	0.669				0.18	0.06
Pebbles					2.05	8.9	0.694				0.08	0.03
Pebbles					2.94	13.0	0.689				0.14	0.04
Pebbles					1.80	8.1	0.679				0.08	0.02
Pebbles					4.47	19.9	0.681				0.15	0.03
Pebbles					3.66	15.6	0.712				0.15	0.05
Narayani												
NAG 48[a]	Bank	December 1995	1		2.76	16.3	0.512	0.543	1.06	1.008	0.13	0.05
PB 54	Susp. materials	July 2005	1	8	2.24	12.9	0.526	0.556	1.06	1.025	0.16	0.06
PB 56	Susp. materials	July 2005	1	4	2.45	13.8	0.539	0.572	1.06	1.015	0.18	0.06
PB 58	Susp. materials	July 2005	1	0	2.86	14.7	0.588	0.614	1.04	1.026	0.23	0.08
Gandak												
BR 336[a]	Bank	May 2004	2		2.26	15.4	0.444	0.545	1.23	1.006	0.14	0.04
BR 335	Clayey bank	May 2004	2		2.39	16.3	0.445	0.578	1.30	1.008	0.19	0.07
BR 117[a]	Bank	August 2001	3		3.14	22.5	0.422	0.507	1.20	1.015	0.14	0.05
BR 113	Susp. materials	August 2001	3	2	2.61	16.4	0.482	0.692	1.44	1.035	0.26	0.10
Gange in Benares												
BR 136	Bedload	August 2001	4		1.78	12.2	0.442	0.513	1.16	1.007	0.08	0.02
BR 137	Susp. materials	August 2001	4	7.9	2.39	14.9	0.486	0.529	1.09	0.993	0.16	0.06
BR 138	Susp. materials	August 2001	4	6	2.51	16.3	0.466	0.591	1.27	1.007	0.21	0.09
BR 139	Susp. materials	August 2001	4	3	2.87	17.5	0.497	0.697	1.40	1.014	0.26	0.12
BR 140	Susp. materials	August 2001	4	1.5	2.75	17.8	0.469	0.771	1.64	1.007	0.27	0.12
Gange in Patna												
BR 124	Bedload	August 2001	5		4.78	39.3	0.369	0.415	1.12	1.061	0.12	0.04
BR 118	Susp. materials	August 2001	5	7.8	1.79	11.1	0.491	0.675	1.38	1.015	0.12	0.04
BR 120	Susp. materials	August 2001	5	3.5	2.41	15.0	0.487	0.648	1.33	1.026	0.21	0.09
BR 122	Susp. materials	August 2001	5	1.5	2.61	17.4	0.455	0.658	1.45	1.021	0.24	0.10

(*continued on next page*)

Table 1 (*continued*)

	Type	Sampling date	Position on the map	Average depth (m)	U (ppm)	Th (ppm)	$(^{238}U/^{232}Th)$	$(^{230}Th/^{232}Th)$	$(^{230}Th/^{238}U)$	$(^{234}U/^{238}U)$	Al_2O_3/SiO_2	Fe_2O_3/SiO_2
Gange in Manihari												
BR 106	Bank	August 2001	6		2.39	20.0	0.362	0.411	1.13	1.030	0.11	0.03
BR 107	Susp. materials	August 2001	6	10.8	2.59	16.6	0.473	0.630	1.33	1.025	0.21	0.09
BR 108	Susp. materials	August 2001	6	5.2	2.39	16.7	0.435	0.651	1.50	1.023	0.25	0.10
BR 109	Susp. materials	August 2001	6	1.5	2.43	17.2	0.429	0.663	1.55	1.025	0.26	0.11

$(^{234}U/^{238}U)$ activity ratios are calculated from measured $^{234}U/^{235}U$ ratios assuming that $^{238}U/^{235}U = 137.88$ and using the following decay constants: $\lambda_{238} = 1.551 \times 10^{-10}\ y^{-1}$ and $\lambda_{234} = 2.823 \times 10^{-6}\ y^{-1}$ (Akovali, 1994; Cheng et al., 2000). $(^{230}Th/^{232}Th)$ activity ratios are calculated from measured $^{232}Th/^{230}Th$ ratios using $\lambda_{232} = 4.948 \times 10^{-11}\ y^{-1}$ and $\lambda_{230} = 9.158 \times 10^{-6}\ y^{-1}$ (Cheng et al., 2000). Analytical uncertainties on the $(^{234}U/^{238}U)$ and $(^{230}Th/^{232}Th)$ ratios are 0.005‰ and 1‰, respectively (2σ error), and yield 1% and 2% for the calculated $(^{238}U/^{232}Th)$ and $(^{230}Th/^{238}U)$ activity ratios, respectively. Al_2O_3, Fe_2O_3 and SiO_2 are expressed in %wt, whereas U and Th are expressed in ppm.

[a] Data from Granet et al. (2007).

This variation is associated to a modification of the mean sediment grain size and to a variation of its mineralogical and chemical composition. The mean particle size increases with depth, with a higher proportion of fine-grained particles (<2 μm) near the surface and a higher proportion of coarse particles (>63 μm) in the bedload sediments. The river bedload is enriched in quartz whereas the mineralogy of suspended load near the surface is dominated by phyllosilicates (micas and clay minerals). This depth dependent granulometrical and mineralogical variations in sediments result in an enrichment in silicon (Si) and a depletion in aluminium (Al) and iron (Fe) in sediments with increasing depth (Galy et al., 2007). The Al_2O_3/SiO_2 and Fe_2O_3/SiO_2 ratios therefore increase with decreasing grain size and sediment depth.

3. ANALYTICAL PROCEDURES

Sediments were dried in the laboratory, and finely crushed by an agate disk mill and then by an agate ball mill. This procedure allows to obtain a grain size small enough to fully digest the sediments, including uranium (U)- and thorium (Th)-rich minerals such as zircons.

Major and trace element concentrations were measured by ICP-AES and ICP-MS at the "Service d'Analyse des Roches et des Minéraux" (CRPG, Nancy) after lithium metaborate fusion. For U and Th analyses of suspended materials, two aliquots of 100 and 50 mg of crushed powder were digested separately for U–Th isotope and concentration analyses, respectively, following a procedure involving HF, HNO_3 and $HClO_4$ acids. Separation and purification of U and Th used a conventional anion-exchange chromatography procedure (e.g., Dequincey et al., 2002; Granet et al., 2007; Pelt et al., 2008). The U and Th isotope ratios were analyzed in Strasbourg (LHyGeS) by Thermal Ionisation Mass Spectrometry on a Thermo Triton using the single Re filament procedure with graphite for U, and a double Re–Re filament assembly for Th. $(^{234}U/^{238}U)$ and $(^{230}Th/^{232}Th)$ activity ratios (parentheses denote activity ratios throughout this article) were calculated from the measurement of $^{234}U/^{235}U$ and $^{232}Th/^{230}Th$ isotope ratios. The accuracy and reproducibility of $^{234}U/^{235}U$ and $^{232}Th/^{230}Th$ measurements were controlled by analyzing the HU1 standard solution and AThO rock standard, respectively. During the data acquisition period, $^{234}U/^{235}U = 0.007566 \pm 10$ ($n = 13$, 2σ error), $^{232}Th/^{230}Th = 182735 \pm 560$ ($n = 5$, 2σ error). The values are consistent with published data (e.g., Sigmarsson et al., 1998; Chabaux et al., 2001; Rubin, 2001; Riotte et al., 2003; Granet et al., 2007). The reproducibility of the Th isotopic analyses was between 0.5% and 1%. It was also assessed by analyzing the BRGM Th105 standard (Innocent et al., 2004) which gives $^{232}Th/^{230}Th = 216751 \pm 860$ ($n = 10$, 2σ error). The measurements were not corrected for mass fractionation as it is small compared to the analytical reproducibility. The mean values for total blanks were lower than 20 pg for U and Th, and remain negligible compared to the U and Th amounts used for analysis (~50 ng for U and ~400 ng for Th). U and Th concentrations in sedi-

ments were measured by isotope dilution on a VG Sector mass spectrometer. The spike is a ^{230}Th and ^{235}U enriched solution that was calibrated with the AThO rock standard. Replicate analyses of several samples yield a U and Th concentration reproducibility better than one percent, indicating that the crushing procedure allows a good and reproducible sample digestion.

4. RESULTS

U–Th data are presented in Table 1 and show that U and Th concentrations in suspended sediments generally decrease with increasing sampling depth (Fig. 2a). Such U–Th systematics can easily be explained by the change of the mineralogical composition of the suspended sediments with depth, namely an enrichment of the sediment with depth in the U and Th-poor quartz relative to phyllosilicates, known to retain U and Th (e.g., Catalano and Brown, 2005; Catalano et al., 2005; Chabaux et al., 2008 and references therein). This is in agreement with previous observations on suspended and bedload sediments from the Amazon basin (Dosseto et al., 2006b). However, U and Th concentrations of bedload and/or bank sediments are not systematically lower than those of suspended sediments collected at the same location (Fig. 2a), which can be due to the presence of heavy minerals like zircon in the bedload. The ($^{238}U/^{232}Th$) and ($^{230}Th/^{232}Th$) ratios in bedload and/or bank sediments are systematically lower than in suspended sediments (Table 1, Fig. 2b and c). Our data also show that all the sediments analyzed for this study exhibit significant ^{238}U–^{234}U–^{230}Th disequilibrium (e.g., Scott, 1968). ($^{230}Th/^{238}U$) activity ratios are systematically higher than unity, with values up to 1.64. This is in agreement with Sarin et al. (1990) who reported values as high as 1.41 for the Ganges river system sediments. ($^{234}U/^{238}U$) activity ratios in all suspended sediments but one (BR 137) are also higher than unity. Values are generally higher or similar to that in bedload sediments. Only Patna bedload sediment (#5, Fig. 1) has a ^{234}U excess over ^{238}U (($^{234}U/^{238}U$) = 1.061) significantly higher than that of the associated suspended materials (($^{234}U/^{238}U$) ranging from 1.015 to 1.026).

For the Narayani River sediments (#1, Fig. 1), ($^{238}U/^{232}Th$) and ($^{230}Th/^{232}Th$) ratios significantly decrease from the surface to the bottom of the water column (Fig. 2b and c) and are positively correlated with Al_2O_3/SiO_2 (Fig. 3a and b) and Fe_2O_3/SiO_2 (not shown) ratios. Data for the Narayani–Gandak sediments define a single trend in a ($^{230}Th/^{232}Th$) vs. Al_2O_3/SiO_2 (or Fe_2O_3/SiO_2) diagram (Fig. 3a), whereas Narayani and Gandak sediments define two separate trends in a ($^{238}U/^{232}Th$) vs. Al_2O_3/SiO_2 (or Fe_2O_3/SiO_2) diagram (Fig. 3b). One trend is defined by Narayani sediments, i.e. sediments collected at the outlet of the Himalaya High Range (#1, Fig. 1), whereas a separate trend is defined by Gandak sediments, further downstream in the alluvial plain (#2 and #3, Fig. 1). This distinction between highland (Narayani) and lowland (Gandak) sediments is also observed in a ($^{230}Th/^{232}Th$) vs. ($^{238}U/^{232}Th$) isochron diagram where the Narayani samples plot along one trend and the Gandak samples along another one (Fig. 3c).

Ganges river sediments (#4–6, Fig. 1) display ($^{230}Th/^{232}Th$) variations similar to that defined by Narayani–Gandak sediments. The Th activity ratios of suspended sediments generally decrease with the increasing depth (Fig. 2c) and are positively correlated with Al_2O_3/SiO_2 ratios according to a trend which is superimposed to that defined by the Narayani–Gandak river sediments (Fig. 4a). The ($^{238}U/^{232}Th$) ratios of the Ganges bedload and/or bank sediments decrease downstream and Ganges suspended sediments plot near those of the Gandak suspended materials in a ($^{238}U/^{232}Th$) vs. Al_2O_3/SiO_2 diagram (not shown). In the ($^{230}Th/^{232}Th$) vs. ($^{238}U/^{232}Th$) isochron diagram (Fig. 4b), Ganges suspended sediments show compositions similar to that of Gandak ones (Fig. 4b). Only one sample (BR 137, #4) collected most upstream plots off this general trend, in between its related bedload sediment and the Narayani sediment trend.

5. DISCUSSION

5.1. Variation of the Th activity ratios and U–Th disequilibria in the river sediments

5.1.1. The Narayani–Gandak river

As presented in the previous section, Narayani–Gandak suspended sediments show one trend of variation in diagrams representing ($^{230}Th/^{232}Th$) vs. major element ratios, whereas two trends appears in diagrams where ($^{238}U/^{232}Th$) is shown. As a first hypothesis, one could suggest that the trend between ($^{230}Th/^{232}Th$) activity ratios and Al_2O_3/SiO_2 (and Fe_2O_3/SiO_2) ratios reflects the variation of these ratios in the source bedrock. In this case, the same relationship should be observed between ($^{230}Th/^{232}Th$) activity ratios and Al_2O_3/SiO_2 (or Fe_2O_3/SiO_2) ratios of the Himalayan source rocks. Pebbles were collected in the Kali Gandaki River catchment, one of the main Himalayan tributaries of the Narayani–Gandak River, and their U/Th ratio was used as a proxy for that of the source bedrock. This assumption is confirmed by the observation that the mean U/Th ratio of the pebbles is very similar to that of Himalayan source rocks as estimated in Granet et al. (2007). Assuming pebbles to be at secular equilibrium, their pebbles ($^{230}Th/^{232}Th$) activity ratios do not show any relationship with Al_2O_3/SiO_2 ratios (Fig. 4a). For this reason, the systematic covariation observed between Th isotope and Al_2O_3/SiO_2 ratios in the Narayani–Gandak river sediments cannot be described in terms of variations in the chemical composition of the Himalayan source rocks.

Galy (2007) proposed that the variation of Al_2O_3/SiO_2 and Fe_2O_3/SiO_2 ratios in sediments of the Ganges river system could be controlled by a mineralogical sorting between coarse sediments, largely constituted by primary minerals, and fine-grained sediments, mainly enriched in clayey secondary minerals. The geochemical variations inferred by such a process are, actually, only little different from those created by a mixing process between two different sedimentary end-members: a coarse-grained one and a fine-grained one. The correlation observed at the scale of the Narayani–Gandak river system between the Th (resp. $^{238}U/^{232}Th$) activity ratios and the Al_2O_3/SiO_2 or Fe_2O_3/SiO_2 ratios

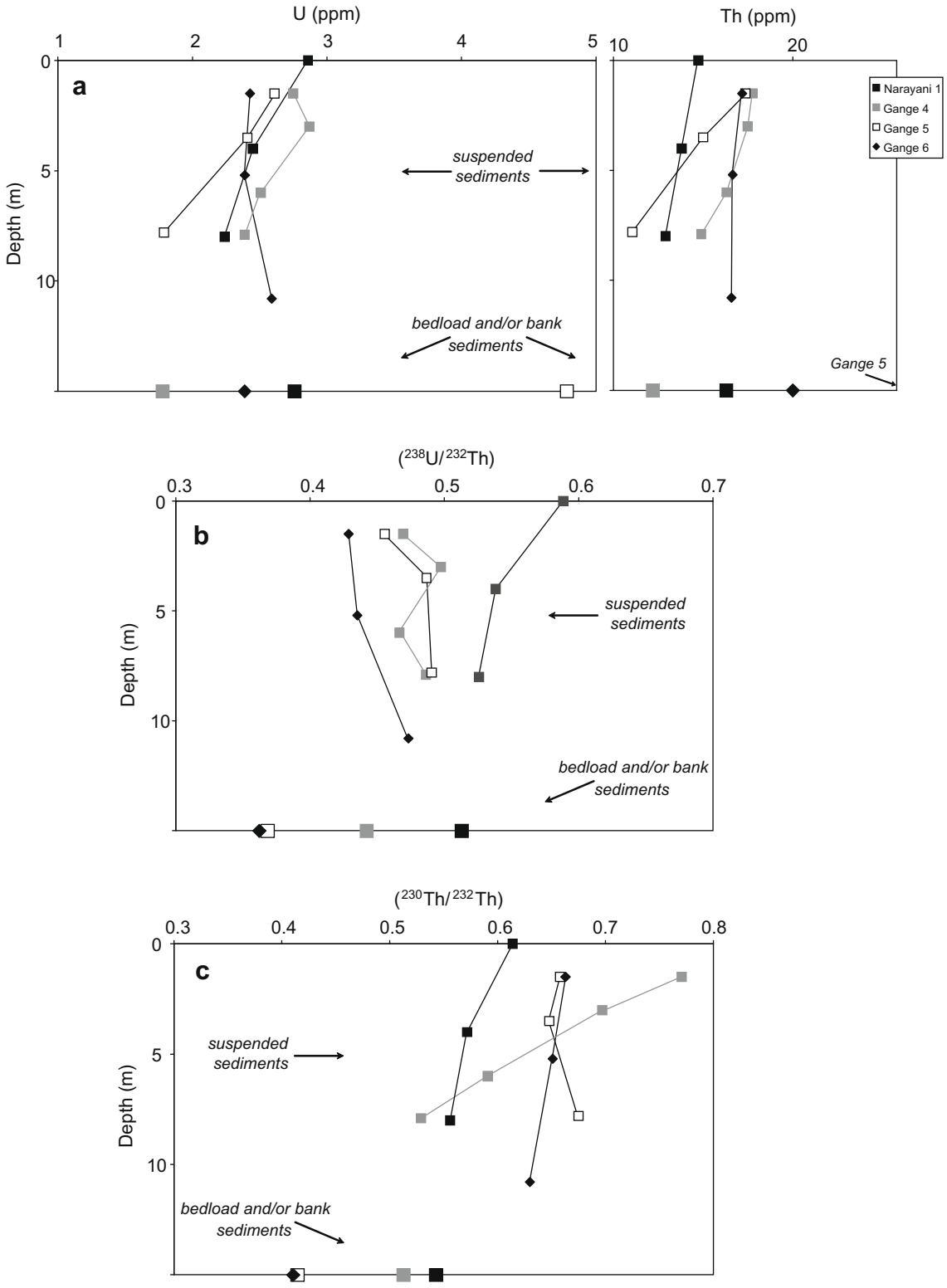

Fig. 2. Depth-variations of (a) U and Th concentrations; (b) ($^{238}U/^{232}Th$) and (c) ($^{230}Th/^{232}Th$) activity ratios for sediments of the Narayani River (black squares) and Ganges River at Benares (grey squares), Patna (white squares) and Manihari (black diamonds).

can be therefore explained by such "mixing" processes between two sedimentary end-members, either genetically related because resulting from a granulometric sorting of a sediment during its transport in the river through the plain, or not directly related because originating from different sources or having different sedimentary histories in

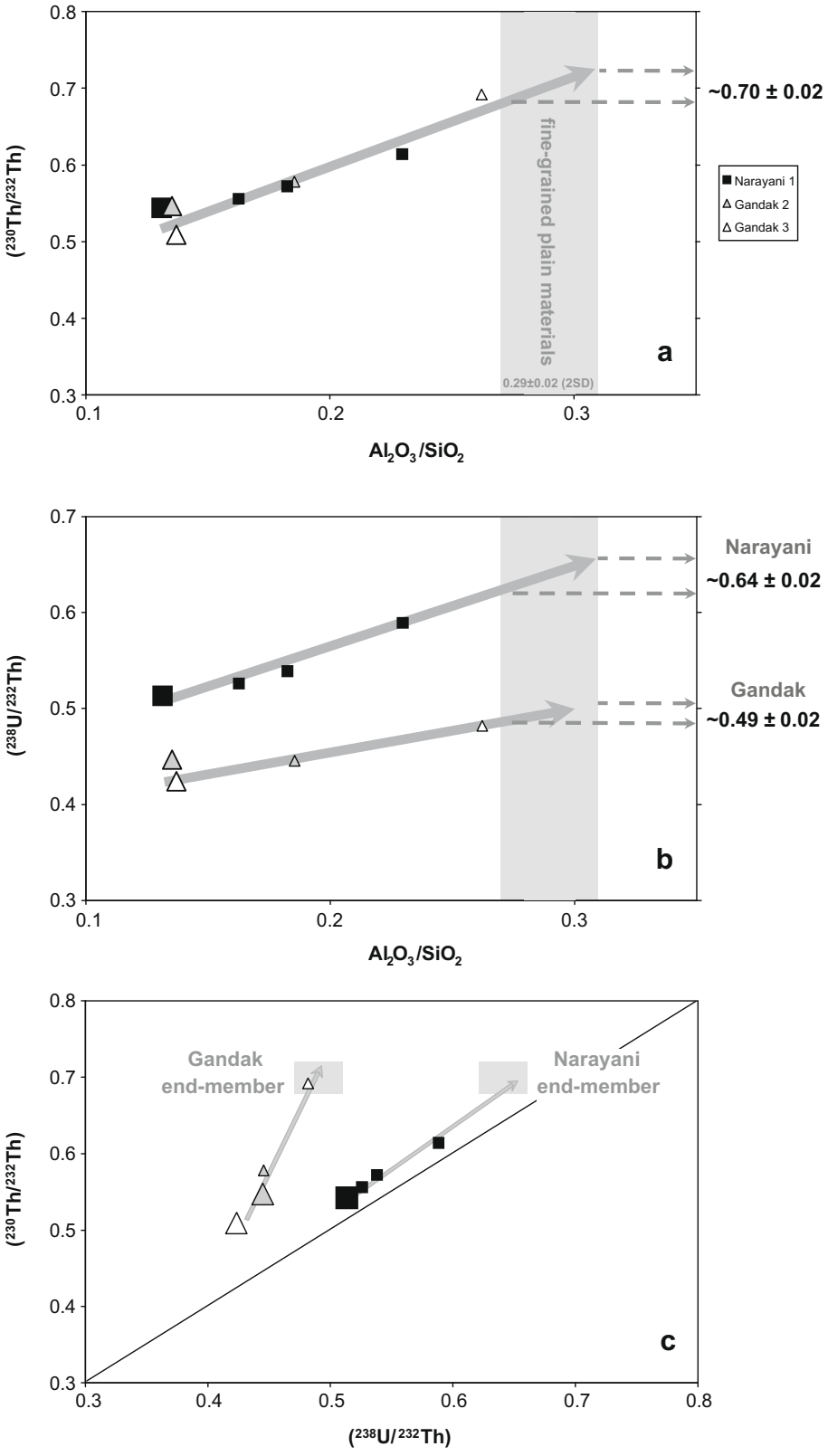

Fig. 3. Plot of the sediment data points in (^{230}Th/^{232}Th) vs. Al_2O_3/SiO_2, (^{238}U/^{232}Th) vs. Al_2O_3/SiO_2, and (^{230}Th/^{232}Th) vs. (^{238}U/^{232}Th) diagrams for the Narayani (black squares) and Gandak (grey and white triangles for the sampling locations #2 and #3 in Fig. 1, respectively) river samples. Larger symbols are used to indicate bedload and bank river sediments, whereas the same but smaller symbols are used to indicate suspended river materials. The Narayani and Gandak fine-grained sedimentary end-members are determined assuming a mixing between coarse-grained materials, marked by bedload and bank sediments, and a fine-grained end-member with $Al_2O_3/SiO_2 \sim 0.29 \pm 0.02$ (2 SD).

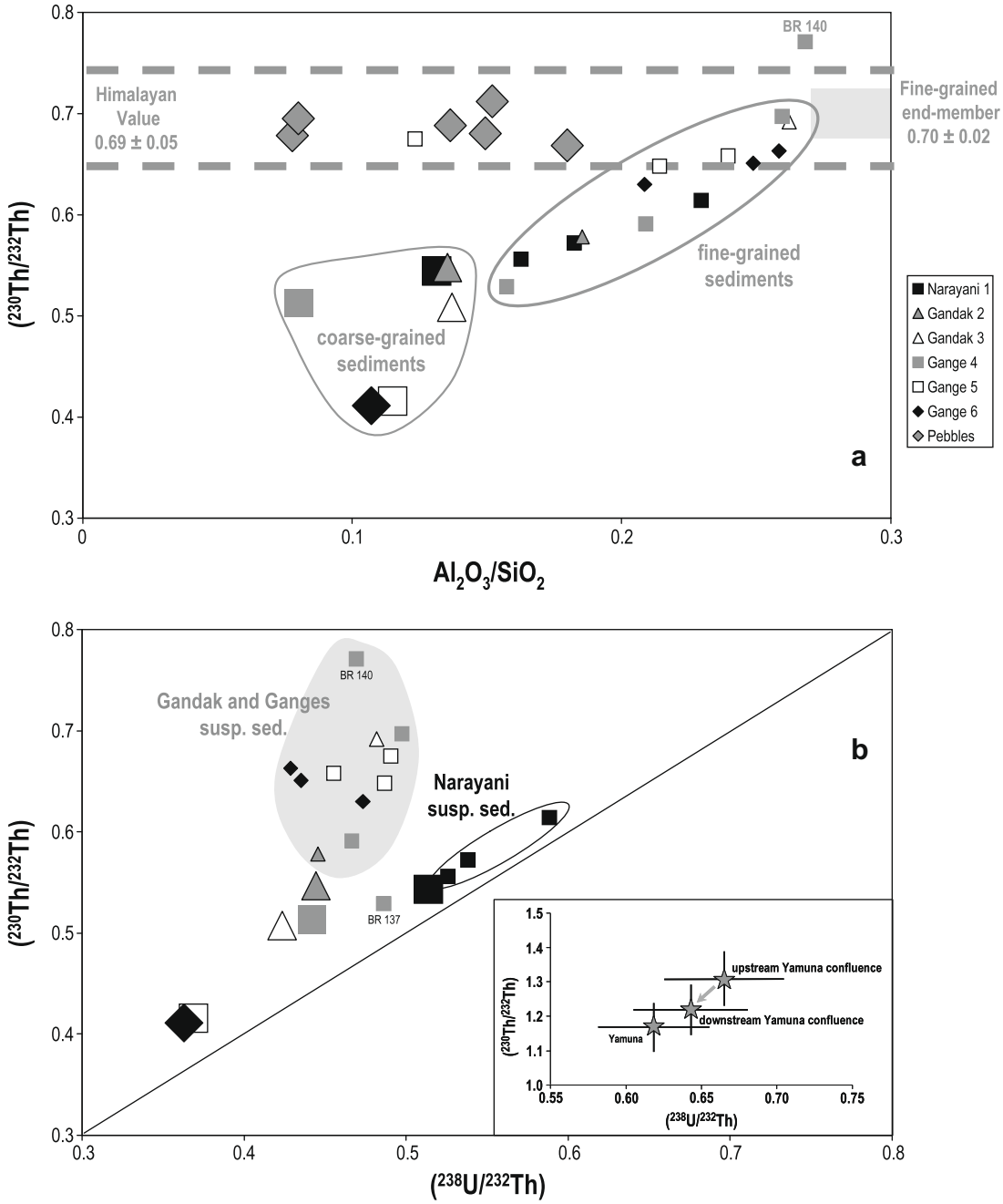

Fig. 4. Plot of the sediment data points in ($^{230}Th/^{232}Th$) vs. Al_2O_3/SiO_2, and ($^{230}Th/^{232}Th$) vs. ($^{238}U/^{232}Th$) diagrams for the Ganges river samples (grey squares, white squares, and black diamonds for the Benares (#4 on the map), Patna (#5 on the map) and Manihari (#6 on the map) sampling locations, respectively). The Narayani and Gandak river samples are plotted with the same symbols as used in Fig. 3. Larger symbols are used to indicate bedload and bank river sediments, whereas the same but smaller symbols are used to indicate suspended river materials. In insert are presented data points of suspended sediments from the Ganges upstream and downstream the Yamuna confluence, and from the Yamuna published in Sarin et al. (1990). A 5% analytical uncertainty is assumed for these data. Such data might suggest that the Yamuna is a significant contributor to the U–Th budget of the suspended sediments carried by the Ganges at Benares.

the plain. Whatever the mixing scenario, the coarse sediment end-member has U–Th characteristics similar to those of bedload or bank sediments of the sampling location. By contrast, the U-series composition of the fine-grained sediment end-member(s) is not known. However, it can be determined using (a) the correlations defined in the ($^{230}Th/^{232}Th$) and ($^{238}U/^{232}Th$) vs. X/SiO_2 diagrams (with X for Al_2O_3 or Fe_2O_3), and (b) realistic values for the Al_2O_3/SiO_2 and Fe_2O_3/SiO_2 ratios of the fine-grained end-members. Major element ratios of the latter end-members can be estimated using average values determined for fine-grained materials from the Gangetic plain: Gomti

River suspended sediments (Singh et al., 2005), clay fractions of floodplain soils (Galy, 2007) and Gangetic plain sediments (Sarin et al., 1989). We obtained $Al_2O_3/SiO_2 = 0.29 \pm 0.02$ (2 SD) and $Fe_2O_3/SiO_2 = 0.12 \pm 0.01$ (2 SD). Using these values, the fine-grained sediment end-members of the Narayani and the Gandak river sediments are found to have very similar ($^{230}Th/^{232}Th$) activity ratios of about 0.70 ± 0.02 (Figs. 3a and c and 5a). The ($^{238}U/^{232}Th$) activity ratios, however, are quite different with an average value of 0.64 ± 0.02 for the fine-grained sediment end-member of the Narayani river and of 0.49 ± 0.02 for that of the Gandak river (Figs. 3b and c and 5a). Such end-member determinations should theoretically be performed by using hyperbolic mixing curves. However it can be easily shown that in the present case, very similar, not to say identical values are obtained by using a simpler linear fitting as done in Fig. 3.

5.1.2. The Ganges river

Most Ganges sediment data points are comprised in the correlation line defined by the Narayani–Gandak sediments in the ($^{230}Th/^{232}Th$) vs. Al_2O_3/SiO_2 diagram (Fig. 4a). Thus, U–Th variations in the Ganges sediments could be interpreted in the same way as for the Narayani–Gandak sediments, namely by mixing between a coarse sediment end-member with a low Th activity ratio and a fine-grained sediment end-member with a higher Th activity ratio. The fact that in the isochron diagram nearly all the data points of the Ganges suspended sediments plot between river bed sediment and the Gandak fine-grained end-member certainly reinforces such an interpretation (Fig. 5a).

In details, however, the U–Th systematic of the Ganges suspended sediments appears to vary as a function of both their depth in the water column and their location in the basin. Thus, at sampling location #4, the U–Th composition of the deeper suspended material (BR 137) can be interpreted as plotting along a mixing trend between its related bedload and/or bank sediment and a fine-grained sediment end-member closed to that defined for the Narayani river (Fig. 5a); the other suspended sediments from deep to intermediate depths, plot along mixing lines between their related bedload and/or bank sediment and the

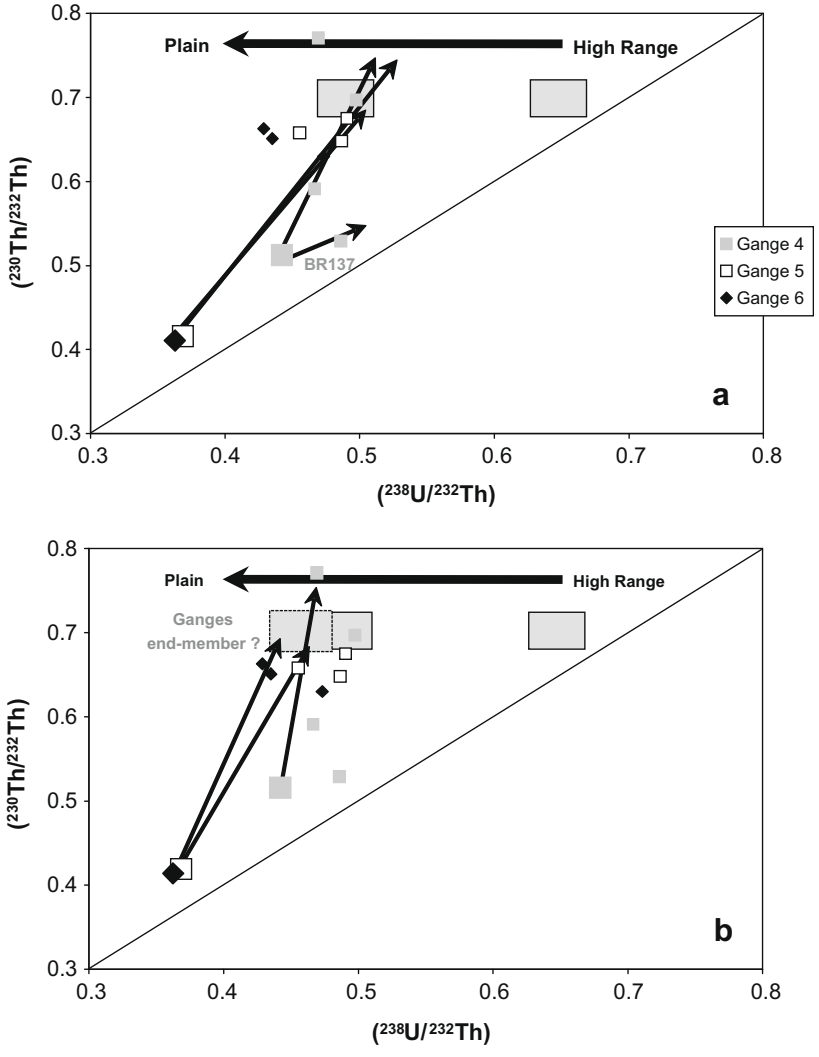

Fig. 5. Plot of the Ganges sediment data points in the ($^{230}Th/^{232}Th$) vs. ($^{238}U/^{232}Th$) diagram showing the downstream U–Th variation of the fine-grained sedimentary end-members from the outlet of the High Range to the plain. Same symbols as in Fig. 4 are used.

fine-grained end-member determined for the Gandak river (Fig. 5a); as for the surface suspended sediments they could plot along slightly different mixing lines between the bedload and/or bank sediments of the sampling locations and a fine-grained material end-member (named the Ganges end-member in Fig. 5b) with a slightly lower ($^{238}U/^{232}Th$) activity ratio but similar Th activity ratio as defined for the Gandak end-member (Fig. 5b).

The U–Th composition of the Ganges sediments could therefore be explained by mixing between a coarse-grained end-member represented by river bedload and/or bank sediments and fine-grained materials, which are marked by different U–Th downstream evolutions in the plain: (1) a decrease of the ($^{230}Th/^{232}Th$) and ($^{238}U/^{232}Th$) activity ratios for the coarse-grained sediment end-member (see also Granet et al., 2007) and (2) a decrease of the ($^{238}U/^{232}Th$) activity ratios without important variation of the Th activity ratios for the fine-grained sediment end-members (Fig. 6). For the fine-grained end-members, the decrease of the ($^{238}U/^{232}Th$) activity ratio is important between the outlet of the High Range (Narayani, #1, Fig. 1) and the plain (Gandak and Ganges, #2–6, Fig. 1) but much more limited among the sampling locations within the Ganges plain. Therefore, the contribution of suspended materials from tributaries (e.g., Yamuna, Son, or Kosi rivers) could result in such small variations of the ($^{238}U/^{232}Th$) activity ratio of the fine-grained end-member within the plain. For instance, Singh et al. (2008) have shown that the Sr and Nd budget of the Ganges sediments at Benares (sampling location #4, Fig. 1), particularly in the fine fraction, is significantly influenced by the contribution of the Yamuna sediments collected just before the confluence with the Ganges, and that this contribution reaches a maximum at Benares and is more negligible downstream. It is important to emphasize that the data of the Ganges and Yamuna sediment samples of Sarin et al. (1990) (collected by the same technique during the same month at Kanpur (upstream Yamuna confluence), at Varanasi (also called Benares, downstream Yamuna confluence) and at Allahabad (Yamuna river)) can point to a similar conclusion for the U–Th budget of the Ganges sediments, namely that the Yamuna sediments can significantly contribute to the U–Th budget of the suspended sediments carried by the Ganges at Benares (insert Fig. 4b). However, since the ($^{238}U/^{232}Th$) and ($^{230}Th/^{232}Th$) variations among these different sediments are small compared to the analytical precision of the techniques used at that time, the above mixing interpretation remains to be confirmed by other new U–Th studies of the sediments carried by the Ganges and its tributaries. Such a work would allow to decipher if the small downstream variations of the ($^{238}U/^{232}Th$) activity ratios in the fine-grained sediment end-members through the alluvial plain have to be ascribed by lateral contribution of sediments from the Ganges tributaries, as suggested by the Sarin et al.'s data, or if they might be linked to a further U–Thfractionation of the fine-grained sediment end-member during its downstream transfer within the plain. We propose in the following to focus on the first order variations observed between the fine-grained sediment end-member at the outlet of the High Range and a mean fine-grained sediment end-member in the plain.

5.2. Origin of the sedimentary end-members and determination of their transfer time

5.2.1. Origin of the sedimentary end-members

It is generally assumed that the materials that compose the alluvial plain ultimately derive from Himalaya Range and not from erosion of a plain substratum. The hypothesis of a Himalayan origin for all the sediments of the plain (bedload, bank as well as suspended sediments) has usually been postulated for interpreting the variations of major

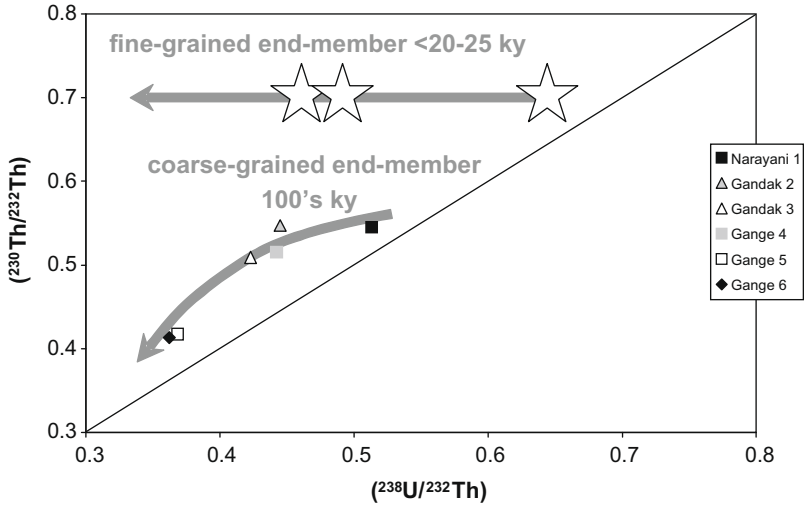

Fig. 6. Interpretative scheme of the downstream evolution of the river sedimentary end-members from the outlet of the High Range to the plain. Coarse-grained and fine-grained sedimentary end-members suffer two different histories of weathering and transfer. The fine-grained river sediments are transferred rapidly as indicated by their rather constant value of Th activity ratios, whereas coarse-grained river sediments are transferred on much longer time-scales as indicated by the significant decrease of their Th activity ratios.

elements in sediments of the Himalaya and Ganges rivers (France-Lanord et al., 2006). For bedload and bank sediments of the Gandak, Ganges and Brahmaputra rivers, this assumption is supported by the similar range of variations of Nd isotopic ratios in these sediments and those in Himalayan rocks (e.g., Singh and France-Lanord, 2002; Granet et al., 2007; Galy et al., 2008; Singh et al., 2008). Such a model explains easily why variations in insoluble element ratios such as Al_2O_3/Fe_2O_3 ratios of all sediments (bedload, bank and suspended materials) analyzed in this study are very close to those measured in Himalayan pebbles (not shown). In the frame of such an interpretation, the contrasted U–Th variation trends observed for the coarse-grained and the fine-grained sediment end-members from upstream to downstream can be explained by three different scenarios: (1) a progressive segregation of these end-members from a common initial Himalayan material through the plain; (2) a significant U–Th atmospheric contribution to the fine-grained end-member in the plain; (3) a different weathering and transfer history of these end-members from Himalaya to the plain.

The first scenario necessitates a mineralogical segregation process with (1) a progressive enrichment of coarse-grained bedload and bank sediments in low Th activity ratio minerals in order to explain the downstream decrease of the Th activity ratio in the coarse-grained sediment end-member in the plain, and consequently, (2) a progressive enrichment of the fine-grained end-member in high Th activity ratio minerals. The Th activity ratios of the fine- and coarse-grained sediment end-members should therefore plot on both sides of that of the initial Himalayan material, here assumed to be represented by the pebbles of the Kali Gandaki river basin. This is clearly not the case since all the sediments analyzed for this study, except one (BR 140, #4, Fig. 1), have ($^{230}Th/^{232}Th$) values lower or equal to the values of pebbles (Fig. 4a). This indicates that the U–Th systematic observed in the river sediments cannot only result from the progressive mineralogical sorting of an initial and single Himalayan sediment. The high Th activity ratio of the BR 140 sediment could result from a local contribution of Yamuna sediments into the Ganges fine-grained sediments at Benares as recently proposed for the Sr and Nd sedimentary budget (Singh et al., 2008).

One might therefore consider that a part of the Th budget of the fine-grained sediments derives from atmospheric contributions. Recent studies indeed show that the input of aeolian dusts influences significantly the budget of some chemical elements like U (Pelt, 2007; Pett-Ridge et al., 2007) and Nd (Kurtz et al., 2001; Dia et al., 2006; Lahd-Geagea et al., 2008). To our knowledge the impact of such an input on the Th budget of soils and river sediments have however never been studied in details and, no direct ($^{230}Th/^{232}Th$) data are available for atmospheric deposits in India. Nevertheless, assuming that aeolian dusts have U–Th characteristics similar to that of loess (e.g., Gallet et al., 1998) or average upper continental crust (UCC) (Taylor and MacLennan, 1985), a ($^{230}Th/^{232}Th$) value comprised between 0.75 and 0.85 can be estimated for atmospheric deposits. Since the Th activity ratios of the fine-grained sediment fractions scatter around 0.7, the above estimates imply that the Th budget of the fine-grained end-member carried by the river sediments is the result of a mixing between the coarse-grained sediment of the sampling site with at least 75% of aeolian inputs when the aeolian material is assimilated to loess-derived materials. This proportion would range from about 40% to 75% (depending on the sampling site) when using the UCC (Taylor and MacLennan, 1985) as the composition of the Aeolian end-member. Thus, regardless the composition chosen for the Aeolian end-member, calculated dust inputs yield unrealistic values, especially if we compare these values with the dust contributions calculated in soil horizons in other geological settings, like in Cameroon (Dia et al., 2006) or Hawaii (Kurtz et al., 2001), which do not usually exceed 10%. For this reason, it is considered that the U–Th composition of river sediments cannot be explained by significant Aeolian inputs and we propose instead a third scenario where both coarse and fine-grained sediment end-members are derived from Himalayan materials but have undergone a different weathering history during transport through the Gangetic plain.

5.2.2. *Transfer time of sediments*

The measurement of U–Th disequilibrium has the potential to bring information on the residence time of the sediments in the river basin. We define the term *sediment residence time* as the amount of time elapsed since sediments were produced from the bedrock. This integrates storage in the weathering profile and subsequent transport in the river, with possible temporary storage in a floodplain. If the *sediment residence time* can be quantified at different locations in the catchment along the river, this can be used to determine the *transfer time* of sediments, i.e. the average time required to transport sediments from a location to another, e.g., through a floodplain. Recent works on the Amazon basin (Dosseto et al., 2006a,b) and on the Ganges river basin (Granet et al., 2007) have highlighted this interest (see also Dosseto et al., 2008a). The determination of such a time information, as well documented in the former studies on the Amazon and Ganges basins, requires first to constrain correctly the U–Th fractionation processes controlling their downstream evolution.

In a previous study (Granet, 2007; Granet et al., 2007), the downstream U–Th isotope variations in the bedload and bank sediments of the Gandak and Ganges rivers were modelled using a U gain and loss model (e.g., Dequincey et al., 2002; Chabaux et al., 2003b; Dosseto et al., 2008b), and it was shown that the transfer time of the Gandak River bedload sediments is about 100 ky between the Himalayan range and the confluence with the Ganges River, and it is of several 100's ky for bedload and bank sediments of the Ganges River between Benares (#4, Fig. 1) and Manihari (#6, Fig. 1). Details of the U gain and loss model are given in Granet et al. (2007).

As underlined in Section 5.1, the U–Th evolution of the fine-grained sedimentary end-members contrasts with that of the coarse-grained end-members as no significant decrease in ($^{230}Th/^{232}Th$) activity ratios is observed whilst ($^{238}U/^{232}Th$) activity ratios decrease from the Himalayas into the plain. A decrease in ($^{238}U/^{232}Th$) is explained by the

preferential mobilization of U over Th as a result of continuous weathering of sediments during their transfer through the catchment. This progressive weathering is supported by major element data which show a downstream increase in weathering intensity, as illustrated by the increasing depletion in Na and K in river sediments (France-Lanord et al., 2006; Galy, 2007). The lack of significant variation of the (^{230}Th/^{232}Th) activity ratios in the fine-grained sediment end-members (0.70 ± 0.02) and the similarity with values observed in Himalayan sediments (0.69 ± 0.05) suggest a recent U–Th fractionation for these sediment end-members, over a short timescale compared to the half-life of ^{230}Th (~75 ky). Application of the uranium gain and loss model (Granet et al., 2007) allows to deduce a maximum time of ~22–27 ky for the transfer of the fine-grained end-member in the Narayani–Gandak river from the outlet of the High Range to the confluence with the Ganges in the Indian plain. A very similar value of about 22–23 ky has been obtained using a simpler two-stage model where we assume first a recent U–Th fractionation and then a decrease of (^{230}Th/^{232}Th) activity ratio by radioactive decay of ^{230}Th (see Appendix). The above estimates give maximum values: much shorter time can be obtained if the Th activity ratios of the suspended sediments are assumed to less decay during the transfer.

On the basis of the above interpretation, it is therefore proposed that the fine-grained and coarse-grained sediment end-members originate from similar sources but have undergone different transfer histories in the plain. The coarse-grained sediment transfer is slow in the plain with a possible long period of pedogenetic maturation in soils and weathering profiles. This scenario is supported by the observation that plain rivers are affected by avulsion processes implying that sediment transfer is driven by alternating periods of transport and deposition (see also Granet et al., 2007). The fine-grained sediment end-member is transferred much faster, and is marked by recent uranium losses. The location where such uranium loss occurs is difficult to constrain on the basis of the present data only. It could occur in the river or in weathering profiles if the fine-grained sediment end-members were also affected by temporary storage in the plain. By looking at the scale of the Narayani–Gandak river, the fine-grained sediment end-member is seen to have (^{234}U/^{238}U) activity ratios around 1.02–1.03. Such a ^{234}U excess can be explained by uptake of uranium from soluble to particulate phases or by its incorporation into secondary phases such as clays. However, since the (^{234}U/^{238}U) activity ratio of the Narayani–Gandak dissolved phase (1.008–1.021; Granet et al., 2007) is not systematically higher than that of the fine-grained end-member it is suggested that the ^{234}U excess of the fine-grained end-member is an inherited soil signature rather than due to a simple U-adsorption process in the river water. Whatever the precise origin and location of the U-loss in the fine-grained materials, the most important point to stress at this stage is that the transfer times of fine-grained sediments and of coarse-grained ones in large watersheds can differ by more than one order of magnitude. Such a variation has certainly to be taken into account for interpreting the contrasted time-scales obtained for the different river systems studied up today.

5.2.3. Consequence for the use of U–Th disequilibria for weathering budgets

Our observations have further consequences for the use of U-series nuclides to assess the steady-state nature of catchment erosion (e.g., Chabaux et al., 2003b, 2008; Dosseto et al., 2008a and references therein). The analysis of U-disequilibria, especially (^{230}Th/^{238}U) disequilibria, in river dissolved and solid phases allows to establish weathering budgets by assuming that the dissolved and solid phases record the whole of the weathering processes undergone by the bedrock initially at secular equilibrium, and hence to assess the steady-state nature of erosion at the watershed scale. This approach has commonly been applied by using only one surface sample of suspended sediments, which is assumed to be representative of the sediment phase carried by the river. In this case it is implicitly assumed that the variability in U-series isotope composition of the river sediment is negligible throughout the water column. Analyses of U–Th disequilibria in the Ganges and Narayani–Gandak sediments emphasize that (^{230}Th/^{238}U) activity ratios in river sediments can be strongly depth dependent with a range of variations that can reach about 40% between the coarse and the surface suspended sediments (Table 1). This clearly outlines that determining the mean value of U-series disequilibria in river sediments is of prime interest before using these geochemical tools in order to assess the steady-state nature of erosion (see also discussion in Dosseto et al., 2006a,b,c, 2008a). Our study of the Ganges river system indicates that a way to constrain such representative value of U-series disequilibria in river sediments is to study the U–Th depth-variations of suspended materials along a stream.

6. CONCLUSION

This study shows significant U–Th disequilibria variations in suspended sediments as a function of sampling depth. Data obtained for samples collected at different locations and water depths in the Ganges and Narayani–Gandak rivers (including their associated coarse sediments) suggest that the U–Th systematic in river sediments can be interpreted in terms of mixing between coarse and fine-grained sediment end-members. We propose in this study that both end-members are originating from Himalayan source, but are characterized by contrasted transfer and weathering histories through the plain. The coarse-grained sediment end-members, represented by river bedload and bank sediments, transit slowly (>several 100's of ky) in the plain. The fine-grained sediment end-member is transferred much faster (<20–25 ky) since uranium loss associated to this transfer is not associated to a significant decrease of the Th activity ratio. The strong dependence of sediment U–Th disequilibria with their sampling depth outlines also the importance of (1) a complete study of the whole granulometric fractions of sediments and (2) a precise quantification of bedload sediment fluxes, for a correct use of U–Th disequilibria to perform mass balance calculations and to assess the steady-state nature of erosion at the scale of a watershed. Studying the U–Th depth-variations

of suspended materials along a stream could present the potential to chemically constrain the representative sediment to be used to avoid biased calculations in such approaches.

ACKNOWLEDGMENTS

M.G. benefited the funding of a Ph.D. scholarship from the French Ministry of National Education and Research. This work was financially supported from the French INSU-CNRS program "Reliefs de la Terre", by the funding from the Région Alsace, France, and the CPER 2003–2006 "REALISE". A.D. is supported by an ARC Future Fellowship. We thank very much the associate Editor S. Krishnaswami for his very constructive and thorough review, which helped to improve the manuscript. We also thank D. Porcelli and two anonymous reviewers for their comments and suggestions. V. Galy and E. Pelt are acknowledged for their help in the field, in the laboratory and for the discussions during the course of this study.

APPENDIX

Mathematical laws describing the behaviour of U and Th isotopes during weathering and transfer processes are required to determine time-scales. Recent studies have shown that complex scenarios involving both gain and loss of U have to be considered during weathering and transfer processes (e.g., Dequincey et al., 2002; Chabaux et al., 2003a,b). In the case of the river sediment studies with U–Th, the scenario used was the scenario detailed in Granet et al. (2007). It is assumed that the abundances of U and Th nuclides in the residual products of weathering (in the present cases river sediments) vary with time according to the following equations:

$$\frac{d^{238}U_{sed}}{dt} = \frac{F_8}{\lambda_8} - k_8{}^{238}U_{sed} \quad (1)$$

$$\frac{d^{234}U_{sed}}{dt} = \frac{F_4}{\lambda_4} + \lambda_8{}^{238}U_{sed} - k_4{}^{234}U_{sed} - \lambda_4{}^{234}U_{sed} \quad (2)$$

$$\frac{d^{230}Th_{sed}}{dt} = \lambda_4{}^{234}U_{sed} - \lambda_0{}^{230}Th_{sed} \quad (3)$$

$$\frac{d^{232}Th_{sed}}{dt} = 0 \quad (4)$$

where the subscript 'sed' refers to sediment; k_8 and k_4 are the U leaching coefficients and represent the fraction of U nuclides released into water per unit of time (t); F_8 and F_4 are the U gain factors and represent the U activity input fluxes per unit of time. λ_8, λ_4 and λ_0 are the decay constants of ^{238}U, ^{234}U and ^{230}Th, respectively. In the present case where ($^{234}U/^{238}U$) is close to equilibrium, it can be noted that the uranium leaching coefficients account for both the preferential leaching and α-recoil ejection of ^{234}U (Chabaux et al., 2008).

This set of differential equations is solved by a Monte-Carlo inversion method which is computed in FORTRAN. It requires to impose a reasonable range of values for the U gain and loss parameters. From literature data, k_8 can be reasonably fixed between 10^{-4} and 10^{-9} y^{-1} (a compilation of U dissolution rates can be found in Dosseto et al., 2008a). The k_4/k_8 ratio is fixed $\geqslant 1$ as ^{234}U is supposed to be more mobile than ^{238}U. The ranges of values for the k_8/F_8 and F_4/F_8 ratios are less constrained. The ratio k_8/F_8 is fixed from 10^{-3} to 10^3, whereas the ratio F_4/F_8, which represents the ($^{234}U/^{238}U$) activity ratio brought to the sediment, is fixed $\geqslant 0.5$ as it allows to recover the values usually observed for waters being in contact with the alteration products. The efficiency of the equation solver was tested by implementing, in our model, previously published U–Th data from Dosseto et al. (2006a). The time-scales calculated with our equation solver are similar to those inferred from the model developed in the latter study. The model has been applied in Granet et al. (2007) to determine the transfer time of bank and bedload sediments of the Ganges Himalayan tributaries. A value of about 100 ky is thus obtained for the transfer of Gandak and Ghaghara river sediments from the outlet of the High Range to the confluence with the Ganges.

In the present study the model is used to estimate the maximum transfer time of the fine-grained end-member in the Narayani–Gandak river from the outlet of the High Range to the confluence with the Ganges in the Indian plain. The ($^{238}U/^{232}Th$) and ($^{230}Th/^{232}Th$) activity ratios of the initial fine-grained sediment retained for this calculation are the highest ratios (i.e., ($^{238}U/^{232}Th$) = 0.66; ($^{230}Th/^{232}Th$) = 0.72 see Fig. 3) estimated for the Narayani fine-grained sediment end-member (#1 in Fig. 1). For the plain sediments, the ($^{238}U/^{232}Th$) and ($^{230}Th/^{232}Th$) activity ratios used are the lowest values (i.e., ($^{238}U/^{232}Th$) = 0.47; ($^{230}Th/^{232}Th$) = 0.68) estimated for the Gandak fine-grained end-member (#3 in Fig. 1). In this case, we obtained $t \sim 22$–27 ky and $k_8 \sim k_4 \sim 1.9 \times 10^{-5}$ y^{-1}.

A similar time (~22–23 ky) is obtained by using a simpler two-stage models, assuming first a U–Th fractionation from ($^{238}U/^{232}Th$) = 0.64 to 0.50 at constant ($^{230}Th/^{232}Th$) = 0.72, and then a decrease of ($^{230}Th/^{232}Th$) by radioactive decay of ^{230}Th, to ($^{230}Th/^{232}Th$) = 0.68.

REFERENCES

Akovali Y. A. (1994) Nuclear data sheets for A = 234. *Nucl. Data Sheets* **71**, 18.

Berner R. A. (1995) Chemical weathering and its effect on atmospheric CO_2 and climate. *Rev. Mineral.* **31**, 565–583.

Catalano J. G. and Brown G. E. (2005) Uranyl adsorption onto montmorillonite: evaluation of binding sites and carbonate complexation. *Geochim. Cosmochim. Acta* **69**, 2995–3005.

Catalano J. G., Trainor T. P., Eng P. J., Waychunas G. A. and Brown G. E. (2005) CTR diffraction and grazing-incidence EXAFS study of U(VI) adsorption onto α-Al_2O_3 and α-Fe_2O_3 (1102) surfaces. *Geochim. Cosmochim. Acta* **69**, 3555–3572.

Chabaux F., Riotte J., Clauer N. and France-Lanord C. (2001) Isotopic tracing of the dissolved U fluxes of Himalayan rivers: implications for present and past U budgets of the Ganges–Brahmaputra system. *Geochim. Cosmochim. Acta* **65**, 3201–3217.

Chabaux F., Riotte J. and Dequincey O. (2003a) U–Th–Ra fractionation during weathering and river transport. *Rev. Mineral. Geochem.* **52**, 533–576.

Chabaux F., Dequincey O., Lévèque J. J., Leprun J. C., Clauer N., Riotte J. and Paquet H. (2003b) Tracing and dating recent chemical transfers in weathering profiles by trace-element geochemistry and ^{238}U–^{234}U–^{230}Th disequilibria: the example

of the Kaya lateritic toposequence (Burkina-Faso). *C. R. Geosci.* **335**, 1219–1231.

Chabaux F., Granet M., Pelt E., France-Lanord C. and Galy V. (2006) ^{238}U–^{234}U–^{230}Th disequilibria and timescale of sedimentary transfers in rivers: clues from the Gangetic plain rivers. *J. Geochem. Explor.* **88**, 373–375.

Chabaux F., Bourdon B. and Riotte J. (2008) U-series geochemistry in weathering profiles, river waters and lakes. In *U/Th Series Radionuclides in Aquatic Systems, Radioactivity in the Environment*, vol. 13 (eds. S. Krishnaswami and J. K. Cochran). Elsevier, pp. 49–104.

Cheng H., Edwards R. L., Hoff J., Gallup C. D., Richards D. A. and Asmerom Y. (2000) The half-lives of uranium-234 and thorium-230. *Chem. Geol.* **169**, 17–33.

Dequincey O., Chabaux F., Clauer N., Sigmarsson O., Liewig N. and Leprun J. C. (2002) Chemical mobilizations in laterites: evidence from trace elements and ^{238}U–^{234}U–^{230}Th disequilibria. *Geochim. Cosmochim. Acta* **66**, 1197–1210.

Dia A., Chauvel C., Bulourde M. and Gérard M. (2006) Eolian contribution to soils on Mount Cameroon: isotopic and trace element records. *Chem. Geol.* **226**, 232–252.

Dosseto A., Bourdon B., Gaillardet J., Maurice-Bourgoin L. and Allègre C. J. (2006a) Weathering and transport of sediments in the Bolivian Andes: time constraints from uranium-series isotopes. *Earth Planet. Sci. Lett.* **248**, 759–771.

Dosseto A., Bourdon B., Gaillardet J., Allègre C. J. and Filizola N. (2006b) Time scale and conditions of weathering under tropical climate: study of the Amazon basin with U-series. *Geochim. Cosmochim. Acta* **70**, 71–89.

Dosseto A., Turner S. P. and Douglas G. B. (2006c) Uranium-series isotopes in colloids and suspended sediments: timescale for sediment production and transport in the Murray–Darling River system. *Earth Planet. Sci. Lett.* **246**, 418–431.

Dosseto A., Bourdon B. and Turner S. P. (2008a) Uranium-series isotopes in river materials: insights into the timescales of erosion and sediment transport. *Earth Planet. Sci. Lett.* **265**, 1–17.

Dosseto A., Turner S. P. and Chappell J. (2008b) The evolution of weathering profiles through time: new insights from uranium-series isotopes. *Earth Planet. Sci. Lett.* **274**(3–4), 359–371.

Dupré B., Dessert C., Oliva P., Goddéris Y., Viers J., François L., Millot R. and Gaillardet J. (2003) Rivers, chemical weathering and Earth's climate. *C. R. Geosci.* **335**, 1141–1160.

France-Lanord C., Galy V., Galy A. and Singh S. K. (2006) Can we derive chemical erosion flux from river sediment?. *Geochim. Cosmochim. Acta* **70**(18 Suppl. 1).

Gallet S., Jahn B., Van Vliet Lanoë B., Dia A. and Rossello E. (1998) Loess geochemistry and its implications for particle origin and composition of the upper continental crust. *Earth Planet. Sci. Lett.* **156**, 157–172.

Galy A. (1999) Etude géochimique de l'érosion actuelle de la chaîne himalayenne. Thèse de l'Institut National Polytechnique de Lorraine.

Galy V. (2007) Transport du carbone organique lors de l'érosion continentale. Thèse du Centre de Recherches Pétrographiques et Géochimiques, Nancy.

Galy V., France-Lanord C., Beyssac O., Faure P., Kudrass H. and Palhol F. (2007) Efficient organic carbon burial in the Bengal fan sustained by the Himalayan erosional system. *Nature* **450**, 407–410.

Galy V., François L., France-Lanord C., Faure P., Kudrass H., Palhol F. and Singh S. K. (2008) C4 plants decline in the Himalayan basin since the Last Glacial Maximum. *Quaternary Sci. Rev.* **27**, 1396–1409.

Granet M. (2007) Constantes de temps des processus d'érosion et d'altération dans le système himalayen: Approche géochimique élémentaire et isotopique par les séries de l'Uranium. Thèse de l'Université Louis Pasteur.

Granet M., Chabaux F., France-Lanord C., Stille P. and Pelt E. (2007) Time-scales of sedimentary transfer and weathering processes from U-series nuclides: clues from the Himalayan rivers. *Earth Planet. Sci. Lett.* **261**, 389–406.

Innocent C., Bollinger C., Chabaux F., Claude C., Durand N., Le Faouder A., Kiefel B. and Pomies C. (2004) Intercomparison of new Th isotopic standards: preliminary results. In *14th Goldschmidt Conference, Copenhagen, Danemark*.

Kurtz A. C., Derry L. A. and Chadwick O. A. (2001) Accretion of Asian dust to Hawaiian soils: isotopic, elemental and mineral mass balances. *Geochim. Cosmochim. Acta* **65**(2001), 1971–1983.

Lahd-Geagea M., Stille P., Gauthier-Lafaye F., Perrone Th. and Aubert D. (2008) Baseline determination of the atmospheric Pb, Sr and Nd isotopic compositions in the Rhine valley, Vosges mountains (France) and the Central Swiss Alps. *Appl. Geochem.* **23**(2008), 1703–1714.

Pelt E. (2007) Mécanismes et constantes de temps des phénomènes d'altération. Thèse de l'Université Louis Pasteur, Strasbourg.

Pelt E., Chabaux F., Innocent C., Navarre-Sitchler A., Sak P. B. and Brantley S. L. (2008) Uranium–thorium chronometry of weathering rinds: rock alteration rate and paleo-isotopic record of weathering fluids. *Earth Planet. Sci. Lett.* **276**, 98–105.

Pett-Ridge J. C., Monastra V. M., Derry L. A. and Chadwick O. A. (2007) Importance of atmospheric inputs and Fe-oxides in controlling soil uranium budgets and behavior along a Hawaiian chronosequence. *Chem. Geol.* **244**, 691–707.

Riotte J., Chabaux F., Benedetti M., Dia A., Gérard M., Boulègue J. and Etamé J. (2003) Uranium colloidal transport and origin of the ^{234}U–^{238}U fractionation in surface waters: new insights from Mount Cameroon. *Chem. Geol.* **202**, 365–381.

Rubin K. H. (2001) Analysis of $^{232}Th/^{230}Th$ in volcanic rocks: a comparison of thermal ionization mass spectrometry and other methodologies. *Chem. Geol.* **175**, 723–750.

Sarin M. M., Krishnaswami S., Dilli K., Somayajulu B. L. K. and Moore W. S. (1989) Major ion chemistry of the Ganga–Brahmaputra river system: weathering processes and fluxes to the Bay of Bengal. *Geochim. Cosmochim. Acta* **53**, 997–1009.

Sarin M. M., Krishnaswami S., Somayajulu B. L. K. and Moore W. S. (1990) Chemistry of uranium, thorium, and radium isotopes in the Ganga–Brahmaputra river system: weathering processes and fluxes to the Bay of Bengal. *Geochim. Cosmochim. Acta* **54**, 1387–1396.

Scott M. R. (1968) Thorium and uranium concentrations and isotope ratios in river sediments. *Earth Planet. Sci. Lett.* **4**, 245–252.

Sigmarsson O., Carn S. and Carracedo J. C. (1998) Systematics of U-series nuclides in primitive lavas from the 1730–36 eruption on Lanzarote, Canary Islands, and implications for the role of garnet pyroxenites during oceanic basalt formations. *Earth Planet. Sci. Lett.* **162**, 137–151.

Singh S. K. and France-Lanord C. (2002) Tracing the distribution of erosion in the Brahmaputra watershed from isotopic compositions of stream sediments. *Earth Planet. Sci. Lett.* **202**, 645–662.

Singh M., Sharma M. and Tobschall H. J. (2005) Weathering of the Ganga alluvial plain, northern India: implications from fluvial geochemistry of the Gomati River. *Appl. Geochem.* **20**, 1–21.

Singh S. K., Rai S. K. and Krishnaswami S. (2008) Sr and Nd isotopes in river sediments from the Ganga Basin: sediment provenance and spatial variability in physical erosion. *J. Geophys. Res.* **113**, 18 p.

Taylor S. R. and MacLennan S. M. (1985) *The Continental Crust: Its Composition and Evolution*. Blackwell Scient. Publ., Oxford, 312 p.

Vigier N., Bourdon B., Turner S. and Allègre C. J. (2001) Erosion timescales derived from U-decay series measurements in rivers. *Earth Planet. Sci. Lett.* **193**, 549–563.

Vigier N., Bourdon B., Lewin E., Dupré B., Turner S., Chakrapani G. J., van Calsteren P. and Allègre C. J. (2005) Mobility of U-series nuclides during basalt weathering: an example from the Deccan Traps (India). *Chem. Geol.* **219**, 69–91.

Walker J. C. G., Hays P. B. and Kasting J. F. (1981) A negative feedback mechanism for the long-term stabilization of Earth's surface temperature. *J. Geophys. Res.* **86**, 9776–9782.

Associate editor: S. Krishnaswami